

Supporting Information

Unprecedented Catalytic Activity of Mn₃O₄ Nanoparticles: Potential Lead of a Sustainable Therapeutic Agent for Hyperbilirubinemia

Anupam Giri,^[a] Nirmal Goswami,^[a] Chandan Sasmal,^[b] Nabarun Polley,^[a] Dipanwita Majumdar,^[c] Sounik Sarkar,^[d] Sambhu Nath Bandyopadhyay,^[b] Achintya Singha,^[c] and Samir Kumar Pal^{[a]*}

^[a]*Department of Chemical, Biological and Macromolecular Sciences, S. N. Bose National Centre for Basic Sciences, Block JD, Sector III, Salt Lake, Kolkata 700 098, India*

^[b]*Department of Obstetrics & Gynaecology, Institute of Post Graduate Medical Education and Research (IPGME&R), 244 A.J.C Bose Road, Kolkata - 700 020, India*

^[c]*Department of Physics, Bose Institute, 93/1, Acharya Prafulla Chandra Road, Kolkata 700 009, India*

^[d]*Department of Biochemistry, University of Calcutta, 35 Ballygunge Circular Road, Kolkata 700 019, India*

Keywords: Mn₃O₄ nanoparticles; Functionalization with organic ligand; Nanocatalysis; Bilirubin decomposition; Hyperbilirubinemia; Whole blood analysis

*Corresponding Authors Email: skpal@bose.res.in

Experimental Section

Chemicals

Human serum albumin (HSA), Trisodium citrate, bilirubin Ix α , sodium hydroxide, manganese chloride, phosphate buffer and MTT based cell viability kit were obtained from Sigma-Aldrich (USA) and used as received without further purification.

Synthesis of Mn₃O₄ NPs

Mn₃O₄ NPs were synthesized by an ultrasound-assisted pathway at room temperature and pressure without the use of any additional surfactants or templates¹. The X-ray diffraction (XRD) patterns of the as-synthesized NPs are shown in Figure S1 in the Supporting Information. All diffraction peaks in the figure is perfectly indexed in the literature to the tetragonal structure of Mn₃O₄ (hausmannite)¹.

Functionalization of as-prepared Mn₃O₄ NPs by different ligands to prepare ligand functionalized-Mn₃O₄ NPs

First, we have prepared 0.5 M citrate (ligand) solution in Milli-Q (from Millipore) water. Then, we have adjusted the pH of the solutions at ~7 by dropwise addition of 1 (M) sodium hydroxide (NaOH) solution. In the ligand solution of pH~7, we have added as-prepared Mn₃O₄ NPs (approximately 100 mg powder Mn₃O₄ NPs in 5 mL ligand solution) and followed by extensive mixing for 12 hours in a cyclo-mixer. Finally, the non-functionalized bigger sized NPs were filtered out (by a syringe filter of 0.22 μ m diameter) and the resulting filtrated solutions were used for our experiments.

Catalytic recyclability

To ensure that the catalyst could be recycled without any significant loss of activity, we started the experiment with 1:1 (10:10 μM) BR: catalyst for first cycle and after every 50 min we added same dose of BR (10 μM) up to 20 dose into the reaction mixture. Keeping the catalyst concentration fixed at 10 μM , BR decomposition kinetics of different cycles was monitored simultaneously using UV-vis spectroscopy.

Characterization techniques

Optical spectra of the solutions were taken with a Shimadzu Model UV-2450 spectrophotometer using a quartz cuvette of 1 cm path length. Circular dichroism (CD) experiments were done in a JASCO 815 spectropolarimeter.

TEM samples were prepared by dropping sample stock solutions onto a 300-mesh carbon coated copper grid and dried overnight in air. Particle sizes were determined from micrographs recorded using a FEI TecnaiTF-20 field-emission high-resolution transmission electron microscope operating at 200 kV.

Raman scattering measurements were performed in a back scattering geometry using a micro-Raman setup consists of a spectrometer (model LabRAM HR, JobinYvon) and a Peltier-cooled charge-coupled device (CCD) detector. An air cooled argon ion laser with a wavelength of 488 nm was used as the excitation light source. Raman spectra of all samples have been recorded at room temperature in the frequency range 50-4000 cm^{-1} .

XRD patterns was obtained by employing a scanning rate of 0.02° s^{-1} in the 2θ range from 10° to 80° by PANalytical XPERT-PRO diffractometer equipped with Cu $K\alpha$ radiation (at 40 mA and 40 kV).

Statistical Analysis: All data expressed in the table as mean±standard deviation, and plotted as mean+ standard error of the mean (SEM). “Statistical significance (*P* value) was determined by using GraphPad Prism version 6.00 for Windows, GraphPad Software, La Jolla California USA, www.graphpad.com”².

Research Donor Blood: Blood specimens were drawn under the ethical guidelines of Research Oversight Committee, IPGME&R, Kolkata (Memo No. Inst/IEC/333), from patients suffering from hyperbilirubinemia, those were not under any medications. 4 mL of blood specimen was drawn from each individual, 2 mL of which was collected in 2 plain VACUETTE vacutainer tubes (1 mL in each tube, for bilirubin and other liver function test parameters) and another 2 mL was collected in tubes containing K₃EDTA (1 mL in each tube, for hemocompatibility test) as anticoagulant.

Determination of total bilirubin and other important parameters in the blood specimens:

50 µL aqueous citrate-Mn₃O₄ NPs solution in phosphate buffered saline (PBS) was added into one portion (~1 mL) of the freshly drawn blood specimen in a vacutainer tube (at a final concentration of 50 µM, biocompatibility of this NP concentration has been confirmed from cell viability assay), another portion of the blood specimen was treated with citrate solution only (as reference), followed by 3 hrs of dark incubation at 2-8 °C. After incubation, to measure the total and conjugated BR content of both the blood specimens (NPs treated and reference), diazotised dichloroaniline has been used for diazo reaction photometry employing a pathological ABL 800 BASIC automated analyser (Radiometer).

In the same blood specimens where we have evaluated total BR level, simultaneously, we have also checked the effects of citrate-Mn₃O₄ NPs on other important parameters including

total protein (Albumin, Globulin), Alkaline Phosphatase, Serum glutamic oxaloacetic transaminase (SGOT), Serum glutamic pyruvic transaminase (SGPT) and GGT (γ -Glutamyltransferase). Furthermore, in order to understand the hemocompatibility of citrate- Mn_3O_4 NPs, we have treated 1 mL blood specimen of each patients in K_3EDTA containing vacutainer tube with NPs solution and other 1 mL with citrate solution (as reference). Haematological parameters pathologically evaluated in this study included Haemoglobin, Total lymphocyte count (TLC), Red blood cell (RBC) count and morphology, Differential count (Neutrophil, Lymphocyte, Monocytes and Eosinophil). Pathological methodologies used for the detection of all these blood parameters are listed below in a tabular form.

List of Tests	Methodology
Total protein	Biuret test
Albumin	Bromocreasol Green
SGOT (AST), SGPT (ALT), γ -Glutamyltransferase (GGT), Alkaline Phosphatase (ALP)	Kinetic UV method based on International Federation of Clinical Chemistry and Laboratory Medicine (IFCC) recommendations
Haemoglobin (Hb)	Automated electronic counter by non-cyanmethaemoglobin method
Red blood cell (RBC) count	Automated electronic counter (based on aperture impedance method/manual)
White blood cell (WBC) count	Automated electronic counter (by haemolysing RBC of diluted blood/manual)
Differential leucocyte count	Leishman stain

Table S1. In vitro effect of citrate-Mn₃O₄ NPs on other liver function parameters of blood specimen. Data are expressed as mean ± standard deviation [n=12]. *P* values were determined by Mann–Whitney test.

Parameters	Reference specimen	NP treated specimen	<i>P</i> Value
Total protein (gm/dl)	6.47±0.90	5.91±0.87	0.22
Albumin (gm/dl)	2.85±1.02	2.43±1.27	0.48
Globulin (gm/dl)	3.62±0.91	3.12±0.89	0.28
SGOT (AST) (U/L)	100.25±76.06	134.12±60.85	0.27
SGPT (ALT) (U/L)	53.75±28.70	133.25±27.62	0.0003
Alkaline phosphatase (U/L)	579.37±823.58	463.37±672.7	0.57
γ-Glutamyl transferase (U/L)	256.62±407.92	213.50±340.16	0.50

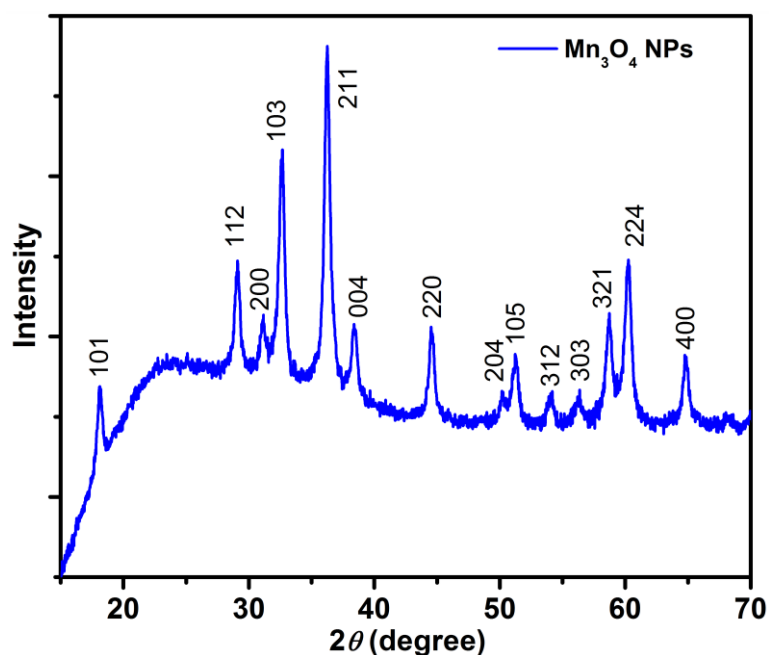


Figure S1. XRD pattern of as-prepared Mn₃O₄ NPs. All diffraction peaks in the figure is perfectly indexed in the literature to the tetragonal structure of Mn₃O₄ NPs (hausmannite).

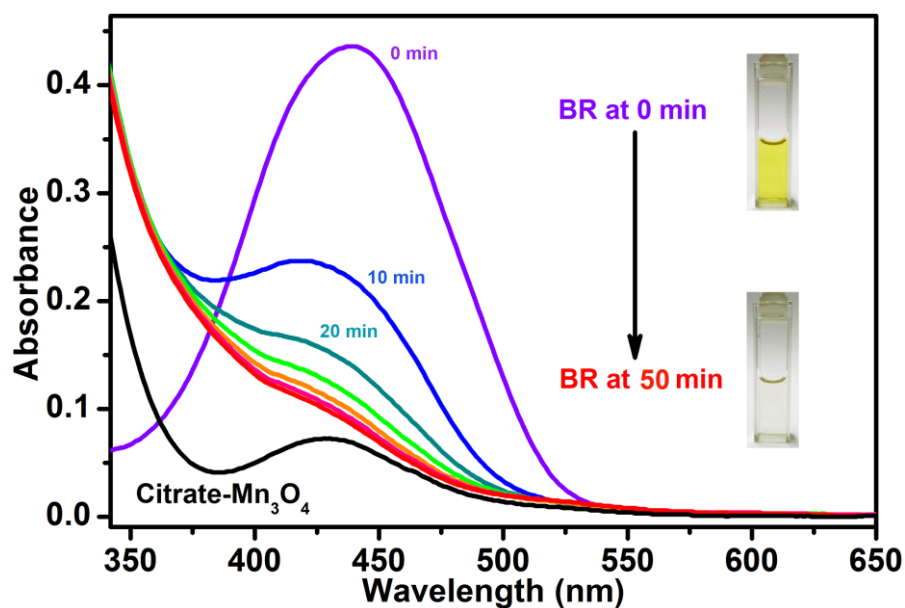


Figure S2. Time dependent UV-vis absorption spectra of BR upon addition of citrate-Mn₃O₄ NPs into the solution. Photographs of the aqueous solution of BR at 0 min and 50 min confirm its decomposition upon interaction with citrate-Mn₃O₄ NPs.

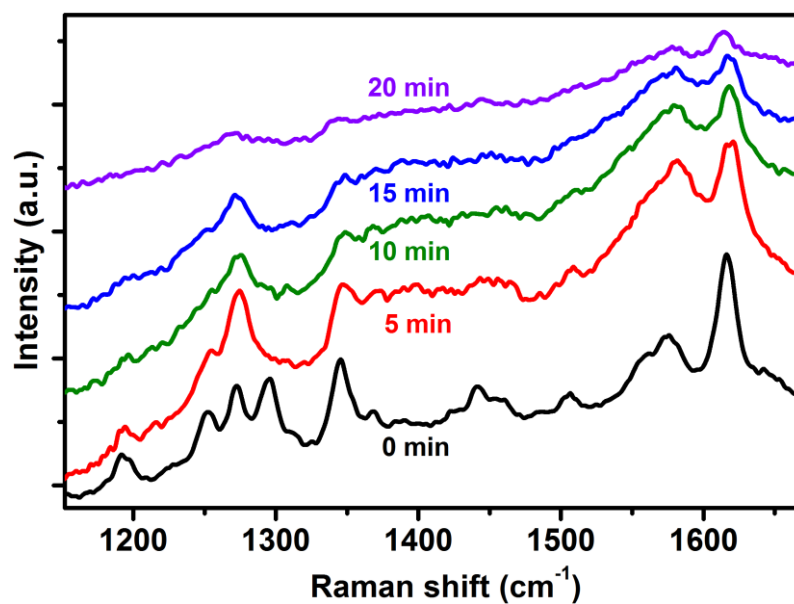


Figure S3. Time dependent Raman study of the aqueous solution of bilirubin (0 min spectrum) in presence of citrate-Mn₃O₄ NPs.

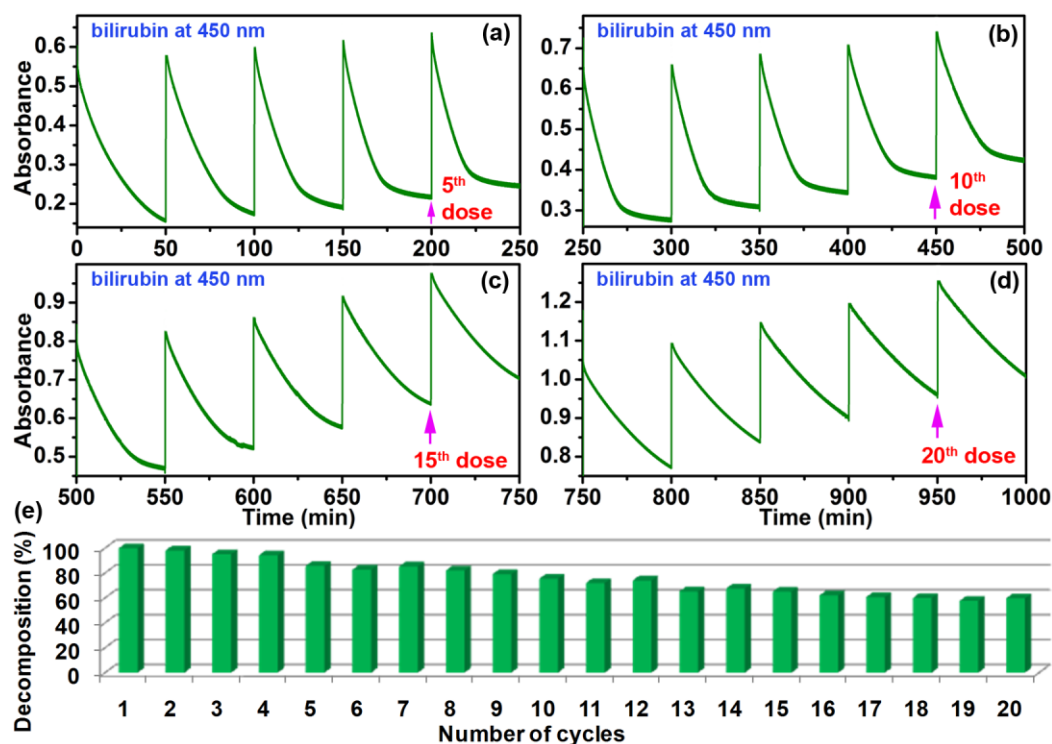


Figure S4 (a-d) shows the cycling curves of bilirubin decomposition kinetics upto 20 cycles. At each 50 minutes interval same dose of bilirubin ($10 \mu\text{M}$) is added into the reaction mixture. (e) Percentage of catalytic decomposition on each cycle. Decomposition of the first cycle has been normalized to 100%.

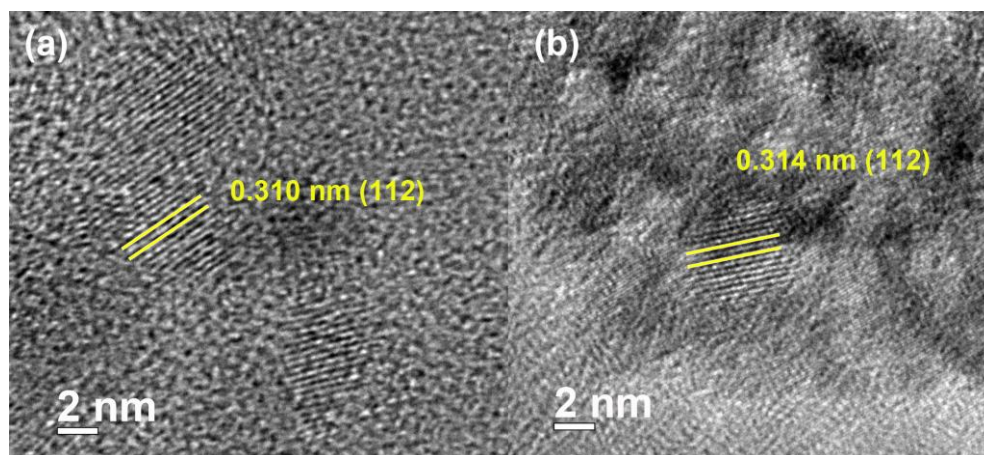


Figure S5. TEM image of citrate- Mn_3O_4 NPs before (a) and after (b) its catalytic performance towards bilirubin decomposition.

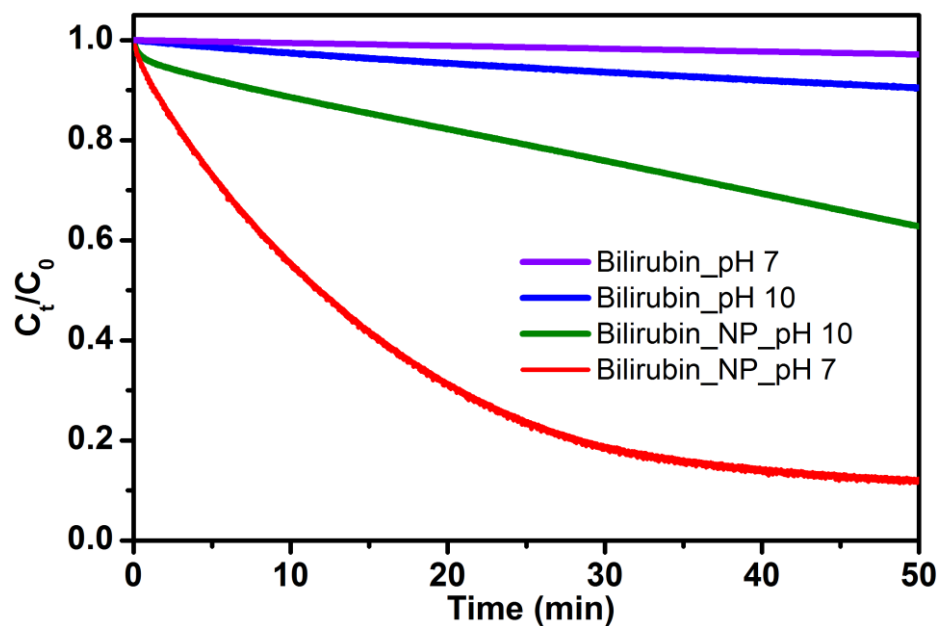


Figure S6. pH dependent catalytic decomposition of the aqueous solution of bilirubin in presence of citrate- Mn_3O_4 NPs. Relative concentration (C_t/C_0) versus time plots for the catalytic decomposition of bilirubin (UV-vis absorbance of bilirubin monitored at 450 nm) in the presence of citrate- Mn_3O_4 NPs are shown.

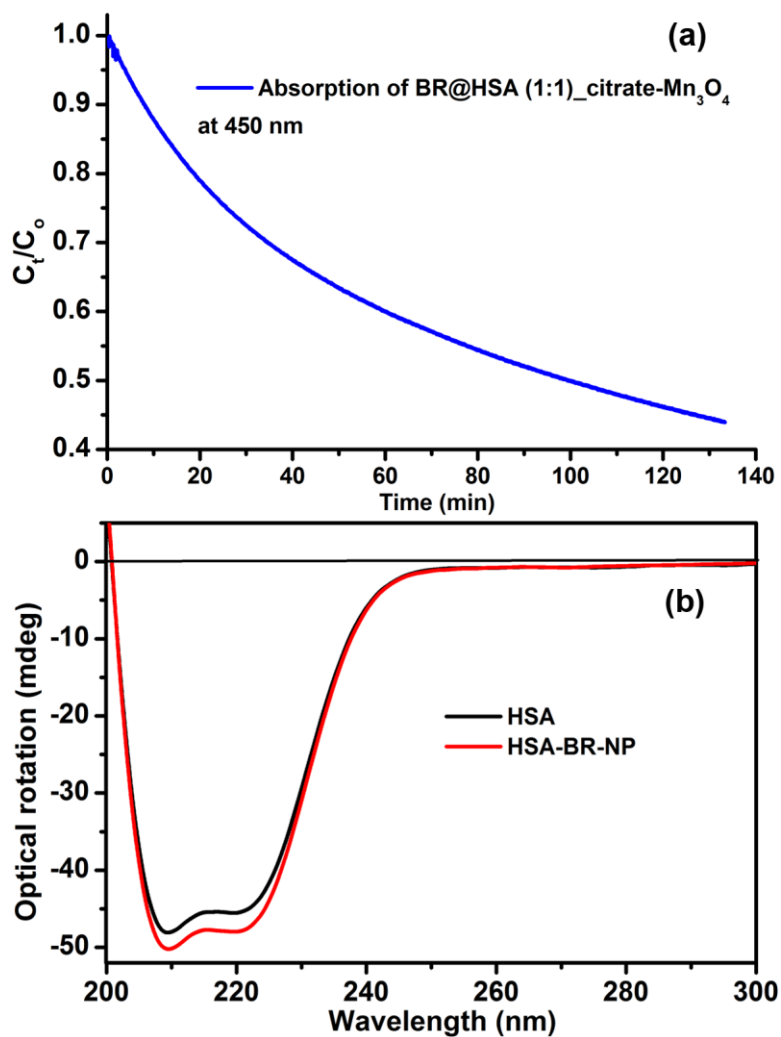


Figure S7. (a) Catalytic decomposition of HSA bound bilirubin (BR) in presence of citrate-Mn₃O₄ NPs. (b) Circular dichroism (CD) spectra of HSA and BR bound HSA after interaction with citrate-Mn₃O₄ NPs. Structural integrity of HSA upon interaction with NP is clearly evident.

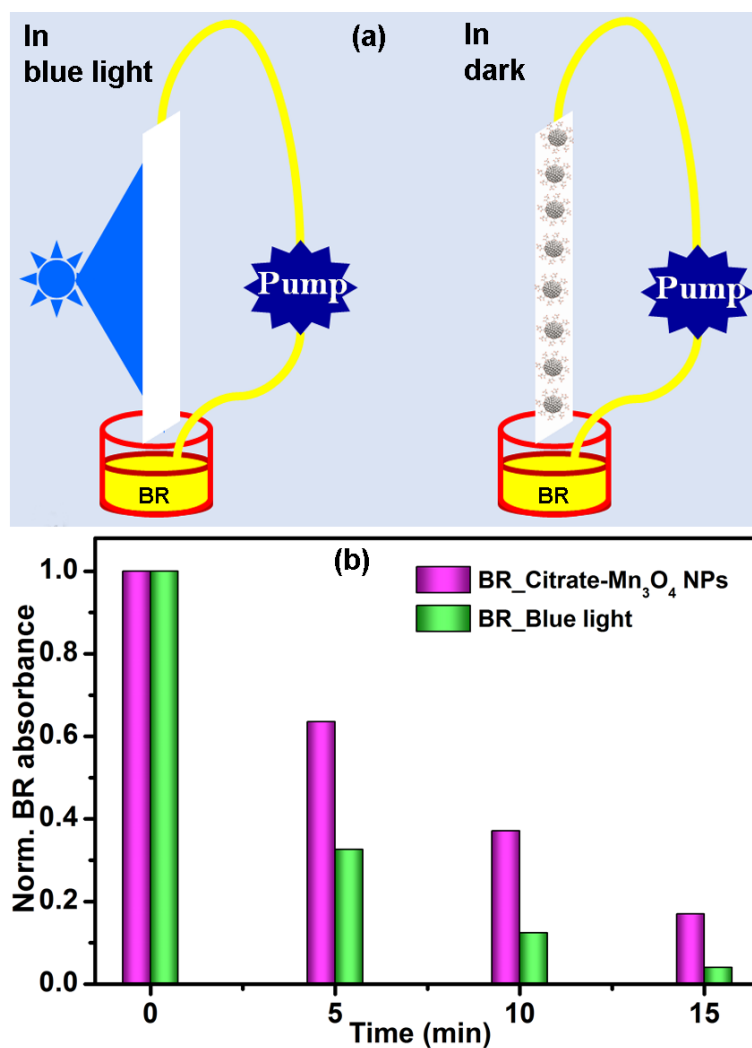


Figure S8. (a) Schematic view of bilirubin decomposition study in presence of blue light (wavelength 460 nm) and citrate-Mn₃O₄ NPs, separately. We have used a strip of chromatography paper to maintain bilirubin flow in both cases. (b) Plots of time dependent UV-vis absorbance of BR in presence of blue light and citrate-Mn₃O₄ NPs (in dark). Proposed potential future use of nanotherapy as an alternative to phototherapy is justified (see text).

References:

- (1) Lei, S.; Tang, K.; Fang, Z.; Zheng, H. *Cryst. Growth Des.* **2006**, *6*, 1757.
- (2) Ondracek, C. R.; McLachlan, A. J. *J. Virol.* **2011**, *85*, 11891.